Domain pattern and piezoelectric response across polymorphic phase transition in strained bismuth ferrite films

H. Y. Kuo,[1] Y. C. Shu,[2,a)] H. Z. Chen,[2] C. J. Hsueh,[2] C. H. Wang,[3] and Y. H. Chu[3]
[1]*Department of Civil Engineering, National Chiao Tung University, Hsinchu 300, Taiwan*
[2]*Institute of Applied Mechanics, National Taiwan University, Taipei 106, Taiwan*
[3]*Department of Materials Science and Engineering, National Chiao Tung University, Hsinchu 300, Taiwan*

(Received 29 October 2010; accepted 19 November 2010; published online 13 December 2010)

A model is developed to investigate the domain pattern and piezoelectric response across the polymorphic phase transition in strained epitaxial bismuth ferrite films. The orientations of stripelike pattern of the mixed rhombohedral and tetragonal phases are predicted as the consequence of competition between elastic and depolarization energies. The abnormally large piezoelectric response is attributed to the strain-driven softening in dielectric stiffness. The results are in good agreement with recent experimental observations and provide a guidance for developing similar strain-driven polymorphic phase transition in other related perovskite material systems. © *2010 American Institute of Physics*. [doi:10.1063/1.3525926]

Bismuth ferrite ($BiFeO_3$) is particularly exciting since it possesses simultaneous ferroelectric and antiferromagnetic orders at room temperature.[1–4] Advances in combining $BiFeO_3$ with ferromagnetic exchange bias make it an ideal candidate for electric control of magnetism.[5] This opens door for the use of multiferroic materials in data storage and spintronics applications. Recently, $BiFeO_3$ has received renewed interest as piezoelectrics since it is lead-free and shows strong piezoelectric response in epitaxial films.[6] This is in sharp contrast to the weak piezoelectric coupling observed earlier in its bulk form.[7] The enhancement in piezoelectricity is attributed to the aggressive strategy of developing the polymorphic phase transition engineered by epitaxial strain imposed by the substrate,[6,8,9] rather than of forming the morphotropic phase boundary by chemical alloying in conventional lead-based ferroelectrics. The rhombohedral and tetragonal phases alternate in layers on a length scale of tens of nanometers in film thickness, forming stripelike patterns with specific orientations and having large piezoelectric responses. However, explanations to the peculiar domain orientations and unusual piezoelectric behavior near the polymorphic phase boundary are still absent and cannot be drawn directly from those proposed for the compositional tailored systems such as the lead zirconate titanate family and relaxors. Here we propose a framework based on the constrained modeling of ferroelectrics[10–12] for resolving these two issues.

Consider a ferroelectric crystal described by two state variables: strain $\boldsymbol{\varepsilon}$ and polarization $\mathbf{p}$. Let $\mathbf{E}^0$ be the applied electric field generated in the absence of the crystal. Under the prescribed electromechanical loading, the state variables $\boldsymbol{\varepsilon}$ and $\mathbf{p}$ can be obtained by minimizing the total free energy by[13–15]

$$\int \{W^{\mathrm{a}}(\mathbf{p}) + W^{\mathrm{elas}}(\boldsymbol{\varepsilon},\mathbf{p}) + W^{\mathrm{d}}(\mathbf{p}) - \mathbf{E}^0 \cdot \mathbf{p}\} d\mathbf{x}, \tag{1}$$

where $W^{\mathrm{elas}}(\boldsymbol{\varepsilon},\mathbf{p}) = \frac{1}{2}[\boldsymbol{\varepsilon} - \boldsymbol{\varepsilon}^*(\mathbf{p})] \cdot \mathbf{C}[\boldsymbol{\varepsilon} - \boldsymbol{\varepsilon}^*(\mathbf{p})]$ and $W^{\mathrm{d}}(\mathbf{p}) = -\frac{1}{2}\mathbf{p} \cdot \mathbf{E}^{\mathrm{d}}$. Above in Eq. (1), the first term is the anisotropy energy density such that the minimization of it over all possible polarizations gives various polarized ground states. The second term is the elastic energy density with $\mathbf{C}$ as elastic moduli and $\boldsymbol{\varepsilon}^*(\mathbf{p})$ as transformation strain. The transformation strains are linked to the polarization by $\varepsilon^*_{ii} = (Q_{11} - Q_{12})p_i^2 + Q_{12}(p_1^2 + p_2^2 + p_3^2)$ if $i = 1,2,3$ and $\varepsilon^*_{ij} = Q_{44}p_i p_j$ if $i \neq j$, where $Q_{ij} = Q_{ji}$ are the electrostrictive coefficients.[16] The strain field $\boldsymbol{\varepsilon}$ can be obtained by solving the mechanical equilibrium equation $\nabla \cdot \boldsymbol{\sigma} = 0$ with stress $\boldsymbol{\sigma} = \mathbf{C}[\boldsymbol{\varepsilon} - \boldsymbol{\varepsilon}^*(\mathbf{p})]$ under appropriate boundary conditions. The third term in Eq. (1) is the depolarization energy density associated with the electric field $\mathbf{E}^{\mathrm{d}}$ generated by the polarization of the material itself. The depolarization field is obtained by solving the Maxwell equation $\nabla \cdot (-\boldsymbol{\epsilon}_0 \nabla \phi + \mathbf{p}) = 0$, where $\mathbf{E}^{\mathrm{d}} = -\nabla\phi$ and $\boldsymbol{\epsilon}_0$ is the permittivity of free space. The final term is the potential energy density due to the applied field $\mathbf{E}^0$. Note that the domain wall energy density is neglected here since the focus here is the domain configuration rather than the domain evolution.

A bismuth ferrite crystal at around room temperature has a stable rhombohedral phase with ⟨111⟩ eight polarized states and a metastable tetragonal phase with ⟨001⟩ six polarized states. The tetragonal phase does not appear naturally in a reference crystal. However, it has been observed to emerge through epitaxial constraint in $BiFeO_3$ films. Indeed, let $\boldsymbol{\sigma}^0$ be the biaxial compressive misfit stress, the superscripts R and T denote rhombohedral and tetragonal phases, and $\mathbf{p}_{\mathrm{s}}^{\mathrm{T}}$ and $\mathbf{p}_{\mathrm{s}}^{\mathrm{R}}$ be the corresponding polarized ground states located at the energy-well points. The equivalent mechanical potential energy density $[-\boldsymbol{\sigma}^0 \cdot \boldsymbol{\varepsilon}^*(\mathbf{p}_{\mathrm{s}}^{\mathrm{T}})]$ from the tetragonal variant polarized normal to the film is negative due to $Q_{11} > 0$ and $Q_{12} < 0$, whereas the contribution from the rhombohedral phase is null since the transformation strain $\boldsymbol{\varepsilon}^*(\mathbf{p}_{\mathrm{s}}^{\mathrm{R}})$ is completely pure shear. As a result, the tetragonal phase might appear if the energy barrier $[W^{\mathrm{a}}(\mathbf{p}_{\mathrm{s}}^{\mathrm{T}}) - W^{\mathrm{a}}(\mathbf{p}_{\mathrm{s}}^{\mathrm{R}})]$ is overcome by the phase difference in mechanical potential energy. This gives polarization oriented normal to the film as a low energy minimizer at sufficiently large compressive misfit stress.

As the $BiFeO_3$ film grows, relaxation of misfit strain provides an opportunity for the emergence of the rhombohe-

a)Author to whom correspondence should be addressed. Electronic mail: yichung@iam.ntu.edu.tw.

dral phase. From the observed microstructure,[6] the pattern of the mixed phase is postulated as a laminate with unknown unit normal **n**. To determine the orientation **n**, the constrained theory of ferroelectric is applied, assuming that the energy-well structure $W^{a}(\mathbf{p})$ is steep away from the ground states.[11,12,17] Thus, each phase is restricted to one of its well points, giving rise to the energy barrier $[W^{a}(\mathbf{p}_s^{T})-W^{a}(\mathbf{p}_s^{R})]$ independent of the laminate orientation **n**. Under these assumptions and from Eq. (1) at the absence of electric field, the determination of **n** depends on the competition between the elastic W^{elas} and depolarization W^{d} energy densities. Indeed, let f denote the volume fraction of the rhombohedral phase. The strain fields $\boldsymbol{\varepsilon}^{R}$ and $\boldsymbol{\varepsilon}^{T}$ can be obtained through strain compatibility, stress equilibrium, and boundary conditions. This gives

$$\boldsymbol{\varepsilon}^{R}=\langle\boldsymbol{\varepsilon}\rangle+(1-f)(\mathbf{a}\otimes\mathbf{n}+\mathbf{n}\otimes\mathbf{a}),$$

$$\boldsymbol{\varepsilon}^{T}=\langle\boldsymbol{\varepsilon}\rangle-f(\mathbf{a}\otimes\mathbf{n}+\mathbf{n}\otimes\mathbf{a}), \tag{2}$$

$$\mathbf{a}=\left(\mathbf{I}-\frac{C_{12}+C_{44}}{C_{12}+2C_{44}}\mathbf{n}\otimes\mathbf{n}\right)[\boldsymbol{\varepsilon}^{*}(\mathbf{p}_s^{R})-\boldsymbol{\varepsilon}^{*}(\mathbf{p}_s^{T})]\mathbf{n},$$

where **I** is the identity, C_{ij} are components of isotropic elastic tensor (Voigt notation), and the notation $\langle\cdots\rangle$ denotes the volume average. Here the plane-stress boundary conditions, $\langle\sigma_{13}\rangle=0$, $\langle\sigma_{23}\rangle=0$, and $\langle\sigma_{33}\rangle=0$, are adopted and the in-plane constraints, $\langle\varepsilon_{11}\rangle=\varepsilon_{11}^{0}$, $\langle\varepsilon_{22}\rangle=\varepsilon_{22}^{0}$, and $\langle\varepsilon_{12}\rangle=0$, are imposed due to biaxial misfit. The depolarization fields $\mathbf{E}^{d,R}$ and $\mathbf{E}^{d,T}$ solved in a way similar to Eq. (2) are

$$\mathbf{E}^{d,R}=\frac{f-1}{\bar{\epsilon}}[\mathbf{n}\cdot(\mathbf{p}_s^{R}-\mathbf{p}_s^{T})]\mathbf{n},$$

$$\mathbf{E}^{d,T}=\frac{f}{\bar{\epsilon}}[\mathbf{n}\cdot(\mathbf{p}_s^{R}-\mathbf{p}_s^{T})]\mathbf{n}, \tag{3}$$

where $\bar{\epsilon}=(1-f)\epsilon^{R}+f\epsilon^{T}$, ϵ^{R} and ϵ^{T} are permittivity coefficients of rhombohedral and tetragonal phases. Note that two assumptions are made in deriving Eq. (3). First, the permittivity of free space in the Maxwell equation is replaced by the permittivity of material for being consistent with the constrained model as described above.[12,18] Second, the permittivity tensor of material is approximated to be isotropic for simplicity. If the anisotropy effect is considered, then the depolarization fields in Eq. (3) remain the same except that the permittivity coefficients are replaced by the projection of permittivity tensors on the direction **n**. But it will not influence the trend that the laminate normal **n** tends to be in the direction for minimizing $[\mathbf{n}\cdot(\mathbf{p}_s^{R}-\mathbf{p}_s^{T})]^2$ due to the reduction of depolarization energy.

The optimal orientation **n** is then readily determined from Eqs. (2) and (3). As explained previously from energy minimization, the tetragonal variant in the two-phase region is $\mathbf{p}_s^{T}=P_s^{T}[001](P_s^{T}[00\bar{1}])$. The rhombohedral variant is taken as $\mathbf{p}_s^{R}=P_s^{R}[111]$, while other choices produce similar results. For bismuth ferrite, spontaneous polarizations $P_s^{R}=0.9$ C m^{-2} and $P_s^{T}=0.55$ C m^{-2}, electrostrictive coefficients $Q_{11}=0.032$ m^4 C^{-2}, $Q_{12}=-0.016$ m^4 C^{-2}, and $Q_{44}=0.01$ m^4 C^{-2}, permittivity constants $\epsilon^{R}=120\epsilon_0$ and $\epsilon^{T}=70\epsilon_0$, and elastic moduli $C_{12}=162$ GPa and $C_{44}=143$ GPa.[16] The observed volume fraction of the rhombohedral phase is $f=0.4$. Under these parameters, the minimum of $(W^{elas}+W^{d})$ occurs at $(\theta,\varphi)=(18°,96°),(18°,354°),(162°,174°)$, and $(162°, 276°)$. Here θ is measured from the normal to the film, and the in-plane angle φ is measured from the [100] axis. The dependence of the elastic, depolarization, and total energy densities of the mixed phase on the in-plane angle φ at $\theta=18°$ is illustrated in Fig. 1. It shows that the elastic energy due to incompatible strains of the mixed phase is minimized at the in-plane angle of 45°, while the depolarization energy is minimized at around 135°. The result that these two angles are almost orthogonal to each other can be shown to be independent of the materials properties including elastic, electrostrictive, and permittivity constants. The optimal laminate orientation is then expected to be within these two angles. Indeed, the calculation shows that the minimum energy occurs at in-plane angles near the [100]/[010] axes. The prediction is in good agreement with that observed in the atomic force microscopy (AFM) image of the mixed phase, as shown in the marked arrows of Fig. 2.[6] These arrows representing the normals to the lamellar patterns of the mixed phase are oriented within 15° around the [100]/[010] axes.

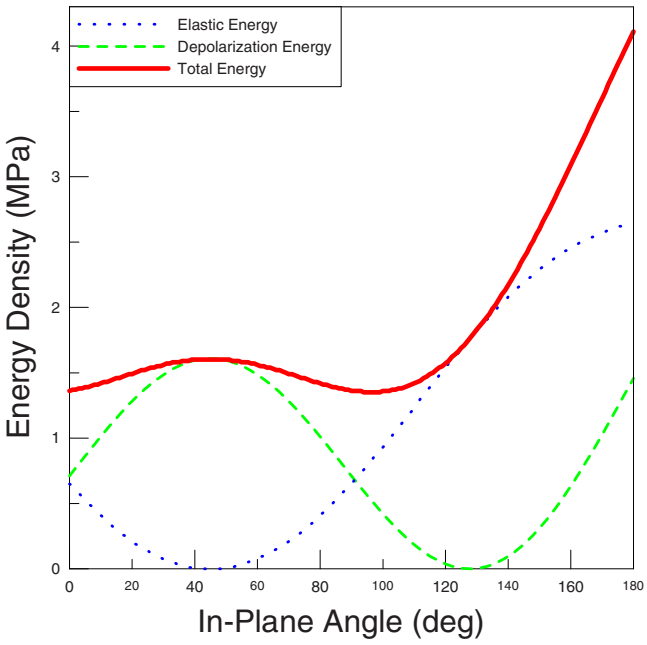

FIG. 1. (Color online) Elastic, depolarization, and total energies of the mixed phase for various laminate orientations. Note that a fixed reference value of energy is taken and removed from the elastic and total energy densities for clearness.

Let us now investigate the piezoelectric response across the polymorphic phase transition in a $BiFeO_3$ film. The out-of-plane displacement has been measured under electric field applied normal to the film. The relevant piezoelectric coupling coefficient is then defined as

$$d_{33}=\frac{d\langle\varepsilon_{33}\rangle}{dE_3^{0}}=\sum_{i=1}^{3}\frac{\partial\langle\varepsilon_{33}\rangle}{\partial p_i}\frac{\partial p_i}{\partial E_3^{0}},$$

$$\langle\varepsilon_{33}\rangle=\langle\varepsilon_{33}^{*}\rangle-\frac{C_{12}}{C_{12}+2C_{44}}[\varepsilon_{11}^{0}+\varepsilon_{22}^{0}-\langle\varepsilon_{11}^{*}\rangle-\langle\varepsilon_{22}^{*}\rangle]. \tag{4}$$

The latter in Eq. (4) is due to the plane-stress argument. The piezoelectric coefficient d_{33} can be achieved once the effec-

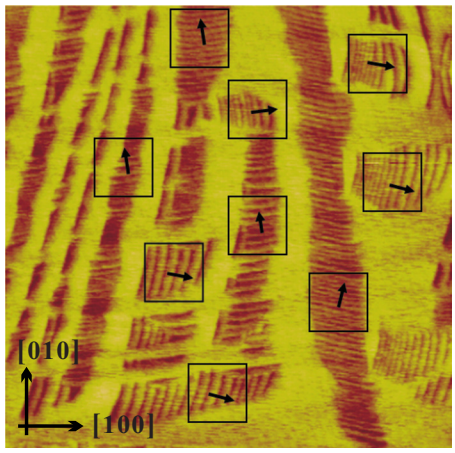

FIG. 2. (Color online) An AFM image showing various lamellar patterns of the mixed R- and T-phases (Ref. 6). The marked arrows denote the directions of in-plane normals to the stripelike patterns. They are oriented within around 15° from the [100]/[010] axes.

tive dielectric constant in the mixed phase is known, and this can be determined by minimizing Eq. (1),

$$\frac{\partial W^{a}(\mathbf{p})}{\partial \mathbf{p}} - \boldsymbol{\sigma} \cdot \frac{\partial \boldsymbol{\varepsilon}^{*}(\mathbf{p})}{\partial \mathbf{p}} - \mathbf{E}^{0} - \mathbf{E}^{d} = 0. \tag{5}$$

The first term in Eq. (5) is explained as the electric field induced by the change of polarization deviating from the polarized ground state. The second term is the effective electric field induced by stress. As evidenced by experiment, polarization in the two-phase region deviates little from its polarized ground state. Thus, the anisotropy energy density is approximated to be $W^{a}(\mathbf{p}) = \frac{1}{2}(\mathbf{p}-\mathbf{p}_{s}^{R}) \cdot (\boldsymbol{\epsilon}^{R})^{-1}(\mathbf{p}-\mathbf{p}_{s}^{R})$ for $\mathbf{p}$ near the R-phase and $W^{a}(\mathbf{p}) = \frac{1}{2}(\mathbf{p}-\mathbf{p}_{s}^{T}) \cdot (\boldsymbol{\epsilon}^{T})^{-1}(\mathbf{p}-\mathbf{p}_{s}^{T})$ for $\mathbf{p}$ close to the T-phase.

Table I shows the piezoelectric coupling coefficients measured from the experiment for pure tetragonal, pure rhombohedral, and the mixed phases in an epitaxial $BiFeO_3$ thin film.[8] The magnitude of d_{33} in the mixed phase is larger than that in the pure tetragonal phase because of the higher relative permittivity in the rhombohedral phase ($\epsilon^{R} > \epsilon^{T}$). Thus, it would be expected that d_{33} of the mixed phase is smaller than that in the pure rhombohedral phase since the effective constant of a mixed phase is bounded by those of the pure phases according to the lamination theory. Surprisingly the mixed phase exhibits abnormally large piezoelectric response than both pure phases. To explain this unusual behavior, consider the stress-induced electric field in the second term of Eq. (5). Its leading coefficient in p_3 is $-\sigma^{0}Q_{12}$, where σ^{0} is the in-plane compressive misfit stress. This term is negative since $\sigma^{0} < 0$ and $Q_{12} < 0$, giving rise to the softening in relative permittivity stiffness (ϵ^{-1}). However, such a softening effect depends on the magnitude of misfit stress which is continuously decreasing as the film grows. As a result, the effect of softening in permittivity stiffness is much more significant in the mixed phase than that in the pure rhombohedral phase, giving rise to higher effective dielectric constant in the mixed phase. Indeed, it is reported that the presence of pure rhombohedral, mixed, and tetragonal phases occurs at compressive misfit strains lower than 3%, between 3% and 4%, and larger than 4%.[6] With these parameters, Table I also lists the piezoelectric coefficients d_{33} obtained from Eq. (4) for pure and mixed phases. The predicted results show the similar trend as those observed in experiment, confirming that the enhancement of piezoelectric response is mainly attributed to the softening in the dielectric stiffness. This softening arises from the electric field induced by stress from the change of out-of-plane polarization.

TABLE I. The comparison between observed and predicted piezoelectric coupling coefficients d_{33} for pure and mixed phases.

d_{33} (pm/V)	Experiment	Prediction
Pure T	28	45
Pure R	61	63
Mixture of R and T	96	116

In summary, a model is developed for predicting the orientations of stripelike domains and explaining the unusual piezoelectric response of the mixed phase in an epitaxial $BiFeO_3$ film. The results show good agreement with experiment and therefore aid the understanding of developing strain-driven polymorphic phase transition in other similar perovskite systems.

We are glad to acknowledge the financial support by the National Science Council, Taiwan under Grant Nos. NSC-98-2221-E-009-095, NSC-97-2221-E-002-125-MY3, and NSC-99-2811-M-009-003.

[1] J. Wang, J. B. Neaton, H. Zheng, V. Nagarajan, S. B. Ogale, B. Liu, D. Viehland, V. Vaithyanathan, D. G. Schlom, U. V. Waghmare, N. A. Spalding, K. M. Rabe, M. Wuttig, and R. Ramesh, Science **299**, 1719 (2003).
[2] C. Ederer and N. A. Spaldin, Phys. Rev. Lett. **95**, 257601 (2005).
[3] G. Catalan and J. F. Scott, Adv. Mater. (Weinheim, Ger.) **21**, 2463 (2009).
[4] J. X. Zhang, D. G. Schlom, L. Q. Chen, and C. B. Eom, Appl. Phys. Lett. **95**, 122904 (2009).
[5] Y. H. Chu, L. W. Martin, M. B. Holcomb, M. Gajek, S. J. Han, Q. He, N. Balke, C. H. Yang, D. Lee, W. Hu, Q. Zhan, P. L. Yang, A. Fraile-Rodriguez, A. Scholl, S. X. Wang, and R. Ramesh, Nature Mater. **7**, 478 (2008).
[6] R. J. Zeches, M. D. Rossell, J. X. Zhang, A. J. Hatt, Q. He, C. H. Yang, A. Kumar, C. H. Wang, A. Melville, C. Adamo, G. Sheng, Y. H. Chu, J. F. Ihlefeld, R. Erni, C. Ederer, V. Gopalan, L. Q. Chen, D. G. Schlom, N. A. Spalding, L. W. Martin, and R. Ramesh., Science **326**, 977 (2009).
[7] J. R. Teague, R. Gerson, and W. J. James, Solid State Commun. **8**, 1073 (1970).
[8] J. X. Zhang, B. Xiang, Q. He, J. Seidel, R. J. Zeches, P. Yu, S. Y. Yang, C. H. Wang, Y. H. Chu, L. W. Martin, A. M. Minor, and R. Ramesh, "A road to huge strains in lead-free multiferroics through nanoscale phase engineering," Nat. Nanotechnol. (submitted).
[9] Z. Chen, L. You, C. Huang, Y. Qi, J. Wang, T. Sritharan, and L. Chen, Appl. Phys. Lett. **96**, 252903 (2010).
[10] Y. C. Shu, J. H. Yen, J. Shieh, and J. H. Yeh, Appl. Phys. Lett. **90**, 172902 (2007).
[11] J. H. Yen, Y. C. Shu, J. Shieh, and J. H. Yeh, J. Mech. Phys. Solids **56**, 2117 (2008).
[12] Y. C. Shu, J. H. Yen, H. Z. Chen, J. Y. Li, and L. J. Li, Appl. Phys. Lett. **92**, 052909 (2008).
[13] Y. C. Shu and K. Bhattacharya, Philos. Mag. B **81**, 2021 (2001).
[14] L. J. Li, J. Y. Li, Y. C. Shu, and J. H. Yen, Appl. Phys. Lett. **93**, 192506 (2008).
[15] L. J. Li, Y. Yang, Y. C. Shu, and J. Y. Li, J. Mech. Phys. Solids **58**, 1613 (2010).
[16] J. X. Zhang, Y. L. Li, Y. Wang, Z. K. Liu, L. Q. Chen, Y. H. Chu, F. Zavaliche, and R. Ramesh, J. Appl. Phys. **101**, 114105 (2007).
[17] R. D. James, J. Mech. Phys. Solids **34**, 359 (1986).
[18] J. Wang and T. Y. Zhang, Appl. Phys. Lett. **88**, 182904 (2006).